Vol 16 No 5, May 2007
1009-1963/2007/16(05)/1276-04
Chinese Physics
© 2007 Chin. Phys. Soc.
and IOP Publishing Ltd

The simulation of temperature dependence of responsivity and response time for 6H-SiC UV photodetector*

Zhang Yi-Men(张义门)†, Zhou Yong-Hua(周拥华), and Zhang Yu-Ming(张玉明)

Key Lab of Ministry of Education for Wide Band-Gap Semiconductor Materials and Devices, Microelectronics Institute, Xidian University, Xi'an 710071, *China*

(Received 22 August 2006; revised manuscript received 25 September 2006)

In this paper the temperature dependence of responsivity and response time for 6H-SiC ultraviolet (UV) photodetector is simulated based on numerical model in the range from 300 K to 900 K. The simulation results show that the responsivity and the response time of device are less sensitive to temperature and this kind of UV photodetector has excellent temperature stability. Also the effects of device structure and bias voltage on the responsivity and the response time are presented. The thicker the drift region is, the higher the responsivity and the longer the response time are. So the thickness of drift region has to be carefully designed to make trade-off between responsivity and response time.

Keywords: 6H-Silicon carbide UV photodetector, absorption coefficient, responsivity, response time
PACC: 0762, 0765E, 7820

1. Introduction

6H-SiC material is a promising candidate for solar-blind ultraviolet (UV) photodetector because of its wide bandgap and good absorption coefficient. 6H-SiC PN junction photodetector has higher responsivity in the wave length range of 300–400 nm and much lower reverse leakage current density than those of GaN.[1] Also it has very low responsivity for infrared ray. So the study of 6H-SiC PN junction photodetector has great prospective significance in the applications to detect ultraviolet intensity up to high temperature with infrared radiation environment, especially for the detection of weak ultraviolet intensity. Furthermore, 6H-SiC has excellent material properties used in the applications of high-temperature and space environments.

Response time and responsivity are very important parameters for characterization of photodetectors and they are related with applied-voltage, structure of device, temperature and so on. Some experimental tests for solar-blind UV photodetector have been made on 6H-SiC.[1,2] They have demonstrated that 6H-SiC UV photodetctor is an attractive device for the detection of wideband ultraviolet intensity. This paper[3] reported the simulation results of 6H-SiC PN junction UV photodetector and it showed the excellent features of this kind UV detector. But there are only few reports related to their temperature dependence.

In this paper, numerical model is presented. For this presented model, the temperature dependence of responsivity and response time of device is simulated and their device structure dependence is discussed. The results show that 6H-SiC PN junction photodetector has excellent temperature stability and it is a good candidate device used in wide temperature range.

2. Model

The two-dimensional Optical Device Advanced Application Module (OD-AAM), drift-diffusion model and recombination model in the MEDICI device-simulator are used. The Poisson equation and continuity equations used in present model are as follows:

$$\begin{cases} \nabla^2\psi = -\rho(x,y,z)/\varepsilon, \\ \dfrac{\partial n}{\partial t} = G_{\rm n} - U_{\rm n} + \dfrac{1}{q}\nabla J_{\rm n}, \\ \dfrac{\partial p}{\partial t} = G_{\rm p} - U_{\rm p} - \dfrac{1}{q}\nabla J_{\rm p}, \end{cases} \tag{1}$$

*Project supported by the National Basic Research Program of China (Grant No 2002CB311904).
†E-mail: ymzhang@xidian.edu.cn

where n and p are electron and hole densities respectively, ψ is potential, ρ charge density, J current density, G generation rate, U recombination rate, and subscript n or p denotes electron or hole respectively. Current density is described by drift and diffusion model, current densities for electrons and holes are expressed as follows:

$$J_{\mathrm{n}} = q\varepsilon\mu_{\mathrm{n}} n + qD_{\mathrm{n}}\nabla n,$$
$$J_{\mathrm{p}} = q\mu_{\mathrm{p}} p\varepsilon - qD_{\mathrm{p}}\nabla p. \tag{2}$$

ε is electrical field strength, μ is the carrier mobility and D is the diffusion coefficient. The following equation can be used for charge density:

$$\rho = q(p - n + N_{\mathrm{D}}^{+} - N_{\mathrm{A}}^{-}), \tag{3}$$

where N_{D}^{+} is the ionized donor concentration and N_{A}^{-} is the ionized acceptor concentration.

The generation rate is related to the incident light beam energy I_{opt}, absorption coefficient α_{opt}, wavelength λ and total quantum efficiency η. It is expressed as:

$$G(x,\lambda) = \eta\left(\frac{\lambda}{hc}\right) I_{\mathrm{opt}}(x,\lambda)\alpha_{\mathrm{opt}}(\lambda), \tag{4}$$

where $I_{\mathrm{opt}}(x,\lambda) = I_{\mathrm{opt}_0}(\lambda)\mathrm{e}^{-\alpha_{\mathrm{opt}}(\lambda)x}$. The total quantum efficiency η is mainly related to external quantum efficiency and here 0.85 is taken. The absorption coefficient α is obtained from the experimental data as shown in Fig.1.

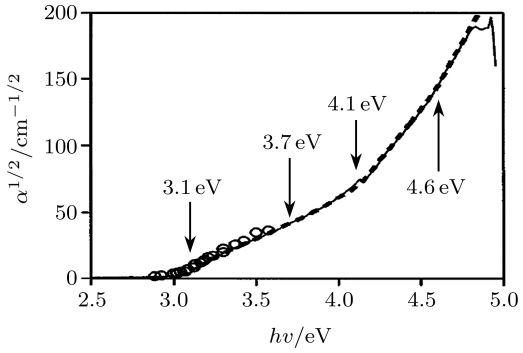


Fig.1. Absorption coefficient vs photon energy. The solid line is from Ref.[4], the dashed line is from Ref.[5] and the open circles are taken from Ref.[6].

The Schokleg–Read–Hall (SRH) recombination model shown in Eq.(5) is used to describe recombination rate U_{n} and U_{p}.

$$U_{\mathrm{SRH}} = \frac{pn - n_{\mathrm{ie}}^2}{\tau_{\mathrm{p}}\left[n + n_{\mathrm{ie}}\exp\left(\dfrac{\Delta E_{\mathrm{t}}}{kT}\right)\right] + \tau_{\mathrm{n}}\left[p + n_{\mathrm{ie}}\exp\left(\dfrac{-\Delta E_{\mathrm{t}}}{kT}\right)\right]}, \tag{5}$$

Here n_{ie} is effective intrinsic carrier concentration, $\Delta E_{\mathrm{t}} = E_{\mathrm{i}} - E_{\mathrm{t}}$, E_{i} is intrinsic energy level and E_{t} is recombination centre energy level, τ_{n} and τ_{p} are electron and hole lifetime respectively. The equations shown in Eqs.(6) and (7) are adopted for τ_{n} and τ_{p} related to doping concentration.

$$\frac{T_{\mathrm{un}}}{\tau_{\mathrm{n}}(x,y)} = A_{\mathrm{n}} + B_{\mathrm{n}}\left(\frac{N_{\mathrm{total}}(x,y)}{N_{\mathrm{SN}}}\right) + C_{\mathrm{n}}\left(\frac{N_{\mathrm{total}}(x,y)}{N_{\mathrm{SN}}}\right)^{D_{\mathrm{n}}}, \tag{6}$$

$$\frac{T_{\mathrm{up}}}{\tau_{\mathrm{p}}(x,y)} = A_{\mathrm{p}} + B_{\mathrm{p}}\left(\frac{N_{\mathrm{total}}(x,y)}{N_{\mathrm{SP}}}\right) + C_{\mathrm{p}}\left(\frac{N_{\mathrm{total}}(x,y)}{N_{\mathrm{SP}}}\right)^{D_{\mathrm{p}}}, \tag{7}$$

where the T_{un}, T_{up} are the SRH lifetime of electron and hole, N_{total} is the total doping concentration, and N_{SN}, N_{SP} the SRH concentration parameters of electron and hole respectively. $A_{\mathrm{n}}, A_{\mathrm{p}}, B_{\mathrm{n}}, B_{\mathrm{p}}, C_{\mathrm{n}}, C_{\mathrm{p}}$ and $D_{\mathrm{n}}, D_{\mathrm{p}}$ are constants. Their values are presented in the Table 1.

Table 1. Parameters used in simulation.[7,8]

T_{un}/s	T_{up}/s	$N_{\mathrm{SN}}/\mathrm{cm}^{-3}$	$N_{\mathrm{SP}}/\mathrm{cm}^{-3}$	A_{n}	A_{p}	B_{n}	B_{p}	C_{n}	C_{p}	D_{n}	D_{p}
1×10^{-6}	6.4×10^{-7}	3×10^{17}	3×10^{17}	1	1	0	0	1	1	0.3	0.3

In addition, incomplete impurity ionization is considered which means that the doped concentration is not completely ionized at room temperature and the ionization rate is raised with the increase of temperature.

3. Results and discussion

Figure 2 shows the cross-section of a p-n junction photodetector. The structure consists of n-type (p-type) substrate with thickness about 300–400 μm, n-type(p-type) 6H-SiC epitaxial layer with thickness about 5 μm, and $p^+(n^+)$ contact layer with depth about 0.2μm. The $p^+(n^+)$ area outside of the $p^+(n^+)$ contact region on the top of the mesa is thinned to 0.1 μm to increase the response for short-wavelength.

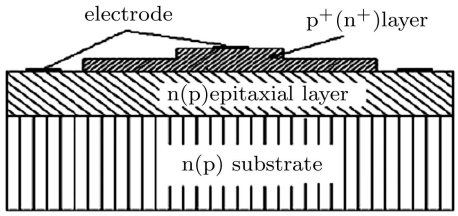


Fig.2. Schematic cross-section of 6H-SiC p-n junction photodetector.

Figure 3 shows the comparison of simulation with experimental data for responsivity of 6H-SiC pn junction photodetector. It can be seen that the simulation results match the experimental data well and this proves that the present model is reasonable.

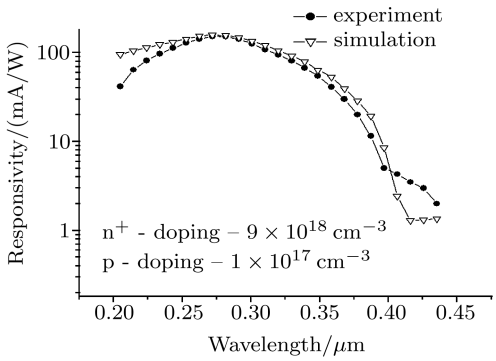


Fig.3. The comparison of simulated responsivity of 6H-SiC pn junction photodetector with experimental data.[9]

The temperature dependence of responsivity and response time for device has been simulated based on above model. The result of responsivity is shown in Fig.4 in the temperature range from 300K to 900 K.

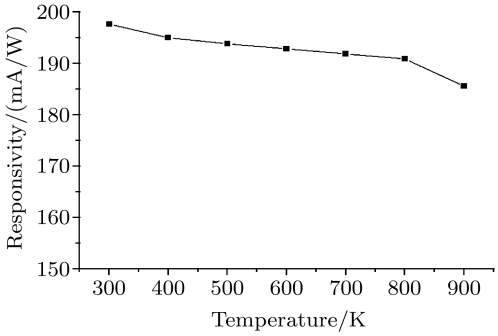


Fig.4. Responsivity vs temperature for 6H-SiC p-n junction photodetector.

We can see from this figure that the responsivity of device decreases gradually from 198 mA/W to 185 mA/W while the temperature changes from 300 K to 900 K. This change is due to the dependence of carrier recombination and carrier mobility on temperature. As the temperature increases, the SRH recombination is enhanced. There are more photon-generated carriers recombined at higher temperature. Meanwhile the carrier mobility and the diffusion length also decrease so that they make the decrease of responsivity.

However the responsivity decreases only about 13 mA/W even though the temperature increment is 600 K. It is seen that the 6H-SiC has good thermal stability for UV photodetection.

Response speed or response time describes the transient behaviour of photodetectors. It is associated with the structure of device and reverse applied-voltage.

Figure 5 shows the transient characteristics of n^+-p junction photodetector. The response time increases from 15 ns to 123 ns as the depth of p-region changes from 10 μm to 80 μm. When the depth of device increases, the carrier drift region also increases. The response time will be longer because of the increase of drift time. So the response speed of device can be speeded-up by thinning the carrier drift region. But the responsivity will be reduced with thinning the drift region, so the design of drift region must make trade-off between the response time and the responsivity.

Response time also varies with applied voltage. Figure 6 shows the changes of response time with voltage for different thickness of epitaxial layer in n^+-p structure. It exhibits that the response time decreases when the applied voltage increases. For the 10 μm and 50 μm p-epitaxial layer devices, the response time decreases from 16.5 ns to 13.8 ns and from 36.9 ns to 35.5 ns respectively as reverse voltage from

0 V to 10 V.

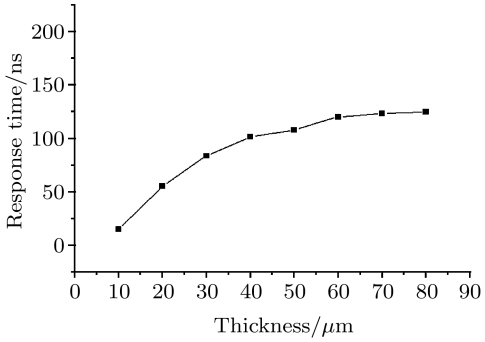


Fig.5. Response time vs thickness of device of 6H-SiC p-n junction photodetector.

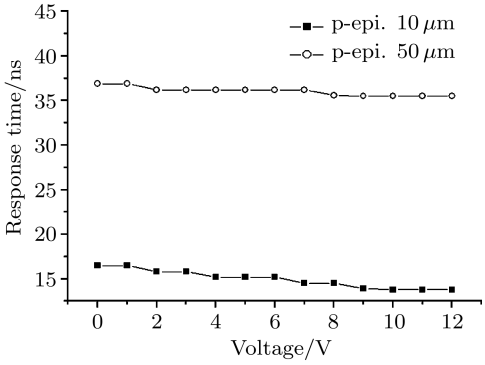


Fig.6. Response time vs voltage for 6H-SiC p-n junction photodetector in different structure. The circles is for 50 μm p-epitaxial layer, the squares is for 10 μm p-epitaxial layer.

As shown in Fig.7, the response time increases from 15 ns to 30 ns in the temperature range from 300 K to 900 K. Carrier mobility decreases with the increase of temperature so that carrier drift time is raised. The response time only changes about 15 ns even though the temperature increment is 600 K. This shows that 6H-SiC UV photodetector has good thermal stability.

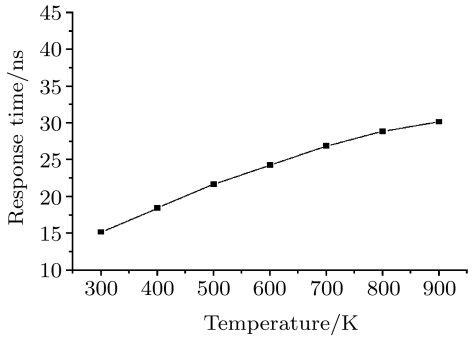


Fig.7. Response time vs temperature for 6H-SiC p-n junction photodetector.

4. Conclusion

The temperature dependence of responsivity and transient characteristics of 6H-SiC p-n junction photodetector is simulated based on the present model. As the simulation results mentioned above, the responsivity and response time of device have a little change with temperature. They are decreased only 13 mA/W and 15 ns respectively when the temperature increases from 300 K to 900 K. 6H-SiC p-n junction UV photodetector has excellent temperature stability and it can be used in the applications of wide temperature range. In addition, the transient properties of this kind photodetector are closely associated with the structure. The responsivity and the response time increase with drift region. It has to make trade-off between responsivity and response time to obtain reasonable drift region. So it is very important to have careful design of structure to improve the performance of photodetector.

References

[1] Torvik J T, Pankove J I and Van Zeghbroeck B J 1999 *IEEE Trans. Electron. Dev.* **46** 1326
[2] Edmond J, Kong H, Suvorov A, Waltz D and Carter C 1997 *Phys. Stat. Sol.* **162** 481
[3] Zhou Y H, Zhang Y M, Zhang Y M and Meng X Z 2004 *Acta Phys. Sin.* **53** 3710 (in Chinese)
[4] van de Lagemaat J, Vanmaekelbergh D and Kelly J J 1998 *J. Appl. Phys.* **83** 6089
[5] Choyke W J and Patrick L 1968 *Phys. Rev.* **172** 769
[6] Philipp H R 1958 *Phys. Rev.* **111** 440
[7] Ruff M, Mitlehner H and Helbig R 1994 *IEEE Trans. Electron. Dev.* **41** 1040
[8] Fujihira K, Tamura S, Kimoto T and Matsunami H 2002 *IEEE Trans. Electron. Dev.* **49** 150
[9] Brown D M, Downey E T, Ghezzo M, Kretchmer J W, Saia R J, Liu Y S, Edmond J A, Gati G, Pimbley J M and Schneider W E 1993 *IEEE Trans. Electron. Dev.* **40** 325